



BIOLOGICALLY BASED UNDULATORY LAMPREY AUV PROJECT

MSEL Report #95-01  
Prepared Under Grant #N00014-94-1-1035

**DISTRIBUTION STATEMENT A**  
Approved for public release  
Distribution Unlimited

Prepared by: Northeastern University  
Marine Systems Engineering Laboratory  
Marine Science Center  
East Point, Nahant Ma 01908

January 1995

19950925 134

**BIOLOGICALLY BASED UNDULATORY LAMPREY AUV PROJECT**

MSEL Report #95-01  
Prepared Under Grant #N00014-94-1-1035

Accesion For	
NTIS	CRA&I <input checked="" type="checkbox"/>
DTIC	TAB <input type="checkbox"/>
Unannounced <input type="checkbox"/>	
Justification _____	
By <i>per btr</i>	
Distribution /	
Availability Codes	
Dist	Avail and/or Special
A-1	

Prepared by: Northeastern University  
Marine Systems Engineering Laboratory  
Marine Science Center  
East Point, Nahant Ma 01908

January 1995

## Table of Contents

<b>1.0</b>	<b>Introduction</b>	<b>1</b>
<b>1.1</b>	<b>Background</b>	<b>1</b>
<b>1.2</b>	<b>Program Goals Phase I</b>	<b>1</b>
<b>2.0</b>	<b>Fish Biomechanic and Kinematic Relationships</b>	<b>2</b>
<b>Figures 1a, 1b</b>		<b>3</b>
<b>Figures 2a, 2b</b>		<b>5</b>
<b>Figure 2c</b>		<b>6</b>
<b>3.0</b>	<b>Summary of Important Biological Relationships</b>	<b>7</b>
<b>Figure 3</b>		<b>8</b>
<b>4.0</b>	<b>Undulatory System Experiments, Results and Analysis</b>	<b>9</b>
<b>4.1</b>	<b>Shape Memory Alloy (SMA) Muscle Mechanism</b>	<b>9</b>
<b>4.2</b>	<b>Single Segment Configuration</b>	<b>9</b>
<b>Figure 4</b>		<b>10</b>
<b>Figures 5a, 5b, 5c, 5d</b>		<b>12</b>
<b>Figure 6</b>		<b>13</b>
<b>Figure 7</b>		<b>14</b>
<b>Figures 8a, 8b</b>		<b>15</b>
<b>4.3</b>	<b>Four Segment Undulatory Experiments</b>	<b>16</b>
<b>4.3.1</b>	<b>Mechanical Configuration</b>	<b>16</b>
<b>4.3.2</b>	<b>Neural Control System</b>	<b>16</b>
<b>Figures 9, 10</b>		<b>17</b>
<b>Figures 11, 12</b>		<b>18</b>
<b>4.3.3 Experimental Setup and Data Acquistion System</b>		<b>19</b>
<b>4.3.4 Experimental Results-Four Segment Undulator</b>		<b>19</b>
<b>Figures 13a, 13b</b>		<b>20</b>
<b>4.3.5 Discussion</b>		<b>21</b>
<b>Figures 14a, 14b</b>		<b>22</b>
<b>Figures 15a, 15b</b>		<b>23</b>
<b>Figures 16a, 16b</b>		<b>24</b>
<b>5.0</b>	<b>Summary of Results and Conclusions</b>	<b>25</b>
<b>6.0</b>	<b>Biological References</b>	<b>27</b>
<b>7.0</b>	<b>Engineering References</b>	<b>28</b>
<b>8.0</b>	<b>Appendix A</b>	<b>30</b>

# BIOLOGICALLY BASED UNDULATORY LAMPREY AUV PROJECT

## PHASE 1

### 1.0. INTRODUCTION

This document serves as the final report for Phase I of this project. The report covers the period from June through December 1994. It includes descriptions of fish biomechanics, kinematic relationships, and neural control concepts. These relationships served as a basis for developing and conducting laboratory experiments aimed at demonstrating the feasibility of creating systems capable of generating smooth undulatory motion similar to that of fish, particularly Lamprey. This report also presents a description of the systems developed, experiments conducted, and the results of these experiments. This work was sponsored by ARPA and ONR under grant number N00014-94-1-1035.

### 1.1 BACKGROUND

There is much to be learned from the way that ocean creatures propel themselves. They have evolved systems which allow them to exhibit complex motion and behavior. During the last two decades substantial progress has been accomplished internationally in understanding some of the basic principles.

Fish use hydrodynamically streamlined bodies to reduce drag and undulatory movement to produce thrust. These movements are generated by alternating muscle contractions on both sides of the body. The rostral (front) segments contract earlier than the caudal (rear) segments. The amplitude of these movements varies along the body and differs between species, but is directly related to the fish form and its rigid and elastic properties. The swimming movements (thrust generating mechanisms) are controlled by a segmental network (spinal pattern generators) whose activity is controlled in a rather simple way (one or two parameters) to produce stereotyped swimming movement. Fish bodies are made up of 24 to over 100 segments of skeletal, muscular, and nervous elements. The problem of mechanical and nerve control can be addressed by reducing the number of degrees of freedom. The mechanical problem is solved by the proper distribution of inertial, elastic, and hydromechanical properties. The nerve problem is solved by the proper coordination of inter-segmental interactions.

### 1.2 PROGRAM GOALS PHASE I

The goal of this phase of the program is to make use of known neural control systems and biomechanical relationships in fish to empirically investigate and demonstrate means of generating smooth undulatory motion similar to that of fish, particularly Lamprey. This phase utilized Shape Memory Alloy (SMA) technology to simulate fish muscles and to provide the needed contrac-

tion mechanism.

## 2. FISH BIOMECHANIC AND KINEMATIC RELATIONSHIPS

As mentioned earlier, significant progress has been achieved during the last two decades in understanding mechanisms of fish swimming. Kinematics, fish muscle activity, synergies of fish myotomes, neural pattern generators and command centers were extensively investigated [references 1 to 26]

Bodyform: The fish body is usually an elongated streamlined form. Length to depth ratios of 4:1 - 6:1 are typical for good swimmers, and are about 10:1 for eel like fish such as Lampreys. The whole fish can be divided into three basic parts: a non-flexible head, an actively flexible middle, and a passively flexible tail.

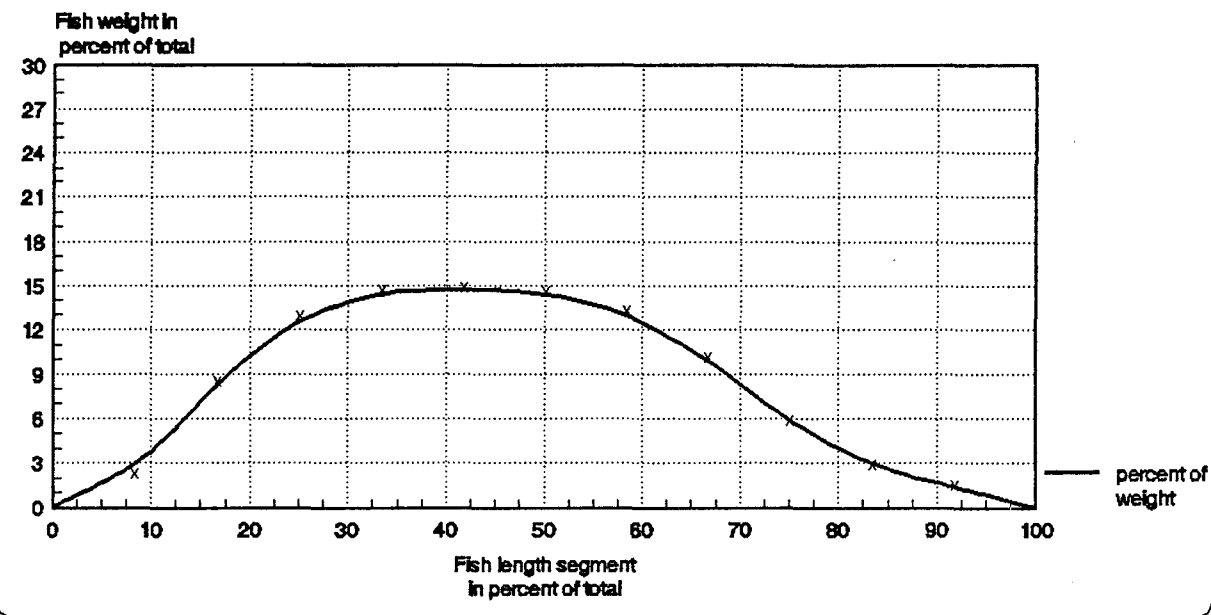
Axial skeletal systems in fish. Stiffness and flexibility of a fish body depends on the axial skeleton which in some fish consists of the bony vertebra column whereas in others it consists of notochord or cartilage. Stiffness is actively controlled by the muscle fiber contractions. We believe that the fish body as a whole is a self-tuning system so that its stiffness is adjusted to the particular frequency of undulation in the range from approximately 0.5 to perhaps 20 hertz for the majority of fishes.

Passive control of fish undulations is determined by the bodyform and particularly by the distribution of its mass along the bodylength. In fish like mackerel, the center of mass is displaced towards the cranial part to about 1/3 of its bodylength, whereas in the eel it is closer to the middle of the bodylength. Figures 1a and 1b are plots of representative data which we measured and which show the relative mass distribution versus body length for these two fish.

Individual segments. Fish musculature and spinal chord are divided into a number of compartments which exactly correspond to the number of vertebrae. Each muscular segment which produces movement consists of left and right myotomes innervated by the ventral roots of the spinal cord which sends commands to the muscle fibers and dorsal roots and which returns information about the produced movement. During swimming activity, segmental pattern generators alternately activate left and right myotomes with half cycle delay between them.

Backbone & Muscles: The mechanical backbone of animals which utilize undulation to generate motion has evolved from the hydrostatic skeleton of invertebrates whose structure permits both undulations and peristalsis to the almost hydrostatic notochord of amphioxus. The latter can change its stiffness by the activation of muscle fibers (paramyosine) lying inside the notochord. The notochord lies along the central axis of the body, contains no bone, and takes up approximately 7% - 10% of the cross sectional area. In Lamprey there is also a cartilaginous vertebra column around the notochord.

**Weight Distribution of Fish**  
**11.5 in long Mackerel**  
**Weight in percent versus length segments**  
**in percent**

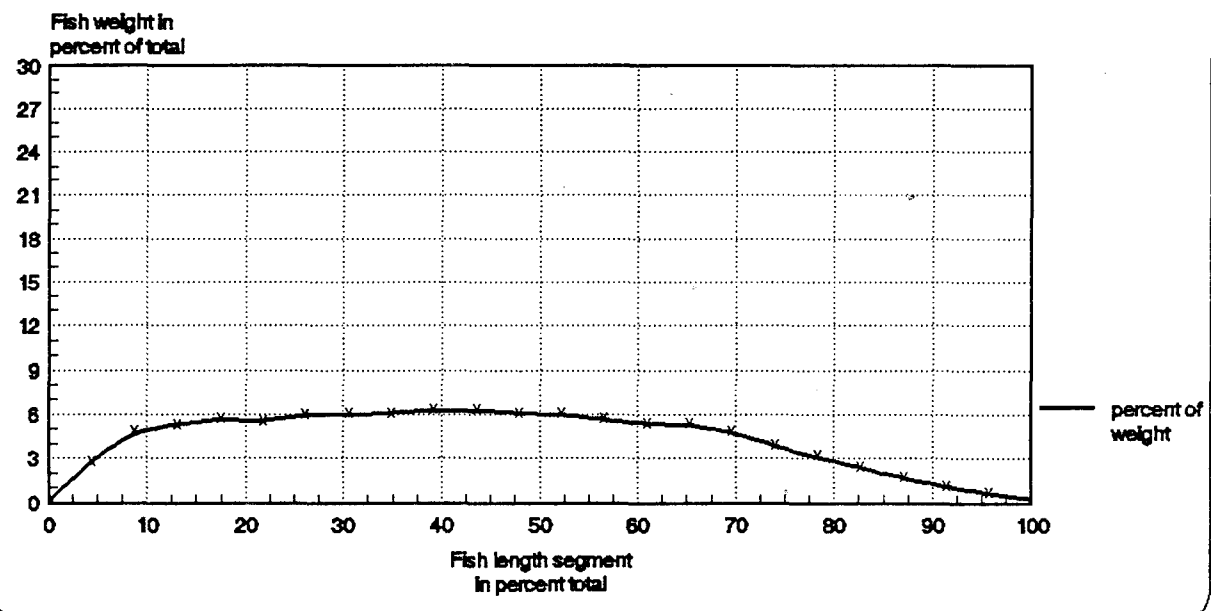


MSEL/NU

MACK2%

Figure 1a

**Weight Distribution of Fish**  
**23 inch long Eel**  
**Weight in percent versus length segments**  
**in percent**



MSEL/NU

EEL%

Figure 1b

The fluid of a hydrostatic skeleton has high internal pressure which can be increased by contracting muscles. The pressure in the notochord of vertebrates is created by cell proliferation during the maturation process. Stiffness is controlled by muscle fiber contractions. Whole body musculature consists of myotomes whose number is equal to the number of vertebra. The final evolutionary stage of increasing stiffness included development of solid bones in teleosts.

In fish as in all animals, movements are produced by the contraction of muscle fibers. Muscle fibers are shortened (contracted) by the commands from motoneurons. One motoneuron usually send axons to a number of muscle fibers, the group of muscle fibers, innervated from one motoneuron, is called 'motor unit'. Each muscle fiber contains a number of miofibrillas (about 300 for a 100 micron diameter). Each miofibrilla consists of a series of sarcomeres. Fish sarcomeres are similar to that of other animals. They are about 2 microns in length and contract in normal conditions from 2 to 5% of their length. Each muscle fiber of 5 mm length (which is typical for adult lamprey or any other fish of average size) therefore contains approximately 100,000 to 1,000,000 sarcomeres and all of them have to be activated synchronously to produce maximal force.

The number of sarcomeres in one cell is so large that, to some extent, it is comparable to the number of crystals in shape memory alloy wires. In these wires a reversible crystalline phase transformation occurs by the application and removal of heat, thereby creating a contraction force similar to that of muscle.

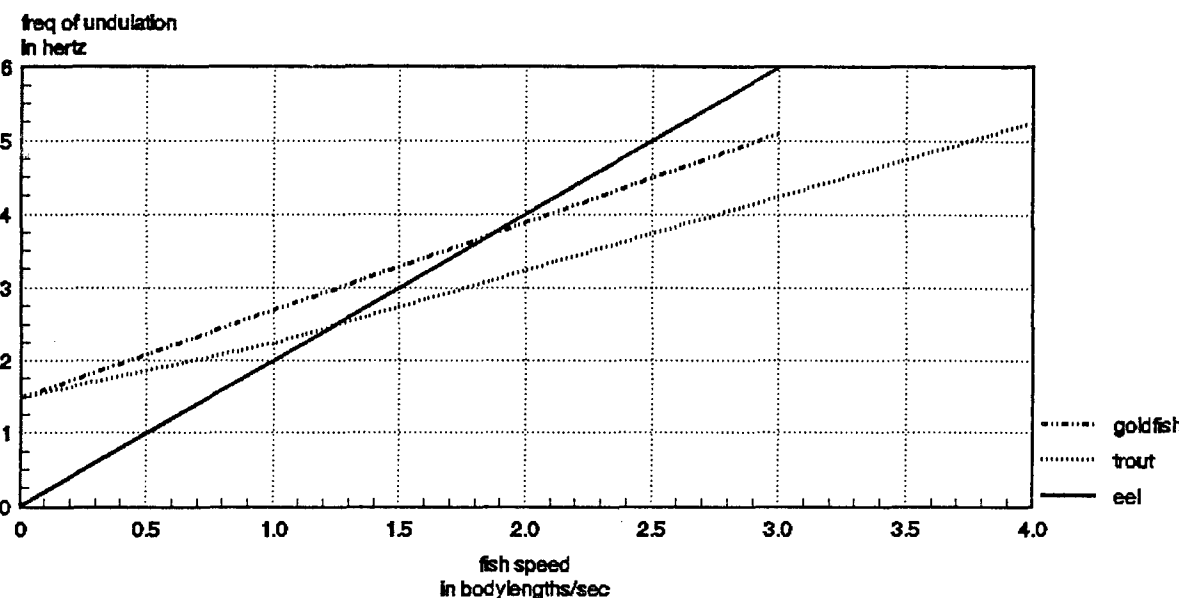
Kinematics. Amplitudes of undulations increase from the snout to the tail in all fish. Low speed movement is controlled by the amplitude of the tail whereas high speed (exceeding 2 bodylength per second) is directly proportional to the frequency of undulations (Figure 2a). The tail motion amplitude is nearly constant for the latter case and is approximately equal to 20% of the bodylength for all studied fishes (Figure 2b).

The flexures of the body usually move backwards along the body and their speed is directly proportional to the speed of swimming (Figure 2c). There is usually one wavelength along the fish body for carangiform type of swimming and 1.25 wavelength for the elongated animals like lamprey or eel.

Coordinations and control. Fish can be considered as an undulating rod in a viscous media. The resonant frequency of the system depends on the interaction of the inertial, elastic, and resistance components. The elastic component can be controlled by muscle force which changes stiffness of the body. The system is possibly self-tuned for a range of undulating frequencies from about 0.5 to 20 hertz for a majority of fish.

The wave of muscular activity propagates along the body due to the time delay in activation of the posterior myotomes in com-

**FREQUENCY OF UNDULATION VERSUS  
SPEED OF SWIMMING**  
for Eel, Trout, and Goldfish  
(Kashin & Smolianinov, 1977)

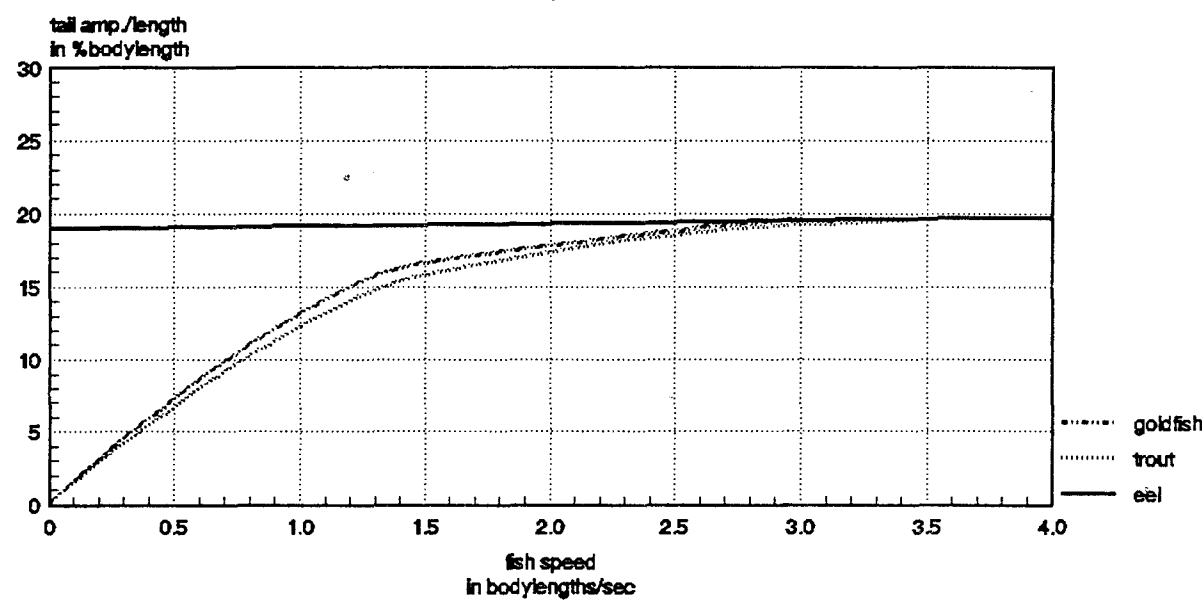


MSEL/NU

Figure 2a

F\_VS\_VL

**TAIL AMPLITUDE MOTION VERSUS  
SPEED OF SWIMMING**  
for Eel, Trout, and Goldfish  
(Bainbridge, 1958)

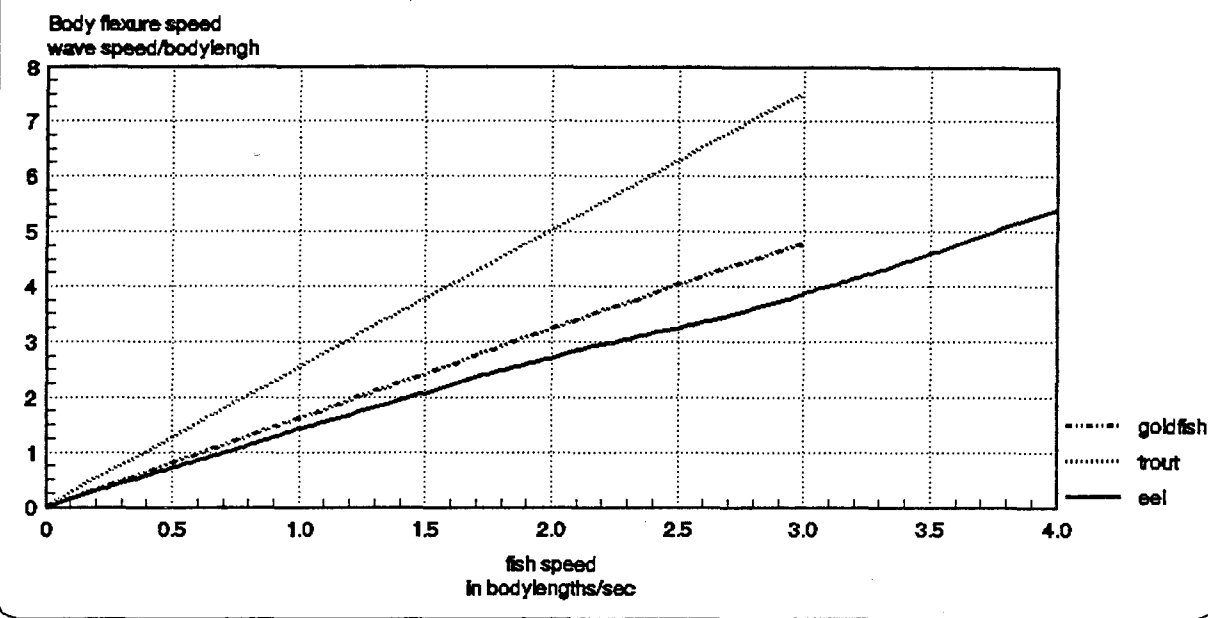


MSEL/NU

Figure 2b

AL\_VS\_VL

**SPEED OF PROPAGATION OF BODY FLEXURES VS  
SPEED OF SWIMMING**  
for Eel, Trout, and Goldfish  
(Bainbridge, 1958)



MSEL/NU

Figure 2c

WL\_VS\_VL

parison with the anterior ones with alternating left and right sides. Although the time delay decreases when the speed of swimming and frequency of undulations increase, its phase lag remains constant so that the time delay is proportional to the cycle duration.

The structure of locomotor cycle in fish in terms of the myotome activations based on electromyographical recordings is shown in Figure 3. Four types of organization or coordination have thus far been described for different species. We will refer to the types of coordination according to the species name for which they were first described.

1. Eel-like or lamprey-like organization of locomotor cycle. Delays between activations of the consecutive myotomes are approximately equal to the delays between ends of their activations (ie  $D_b = D_e$ ). The activation delay is approximately equal to the cycle duration  $T$  divided by the number of segments on a given side. Approximately one fourth of all ipsilateral myotomes are active at any given moment of time.

2. Carp locomotor cycle. Delays between activations and deactivations of consecutive myotomes are shorter than those in Case 1 above. As a result there is a larger percentage activation than in the first case at any moment of time while swimming.

3. Trout locomotor cycle. This is similar to the first case in terms of delay between activations, however, the myotome burst durations decrease from the snout to tail ( $Tact1 > Tact2 > Tactn$ ).

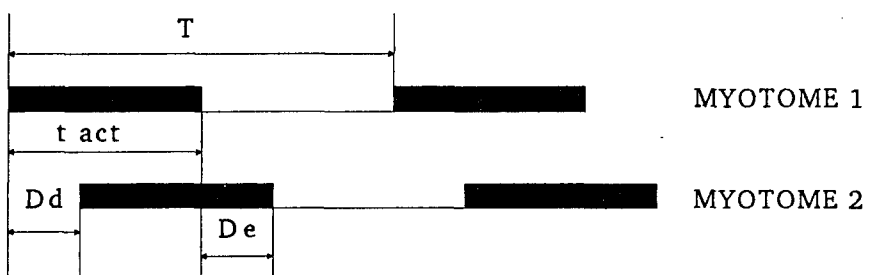
4. Shark locomotor cycle. The phase delay between activations of myotomes is equal to the burst duration of the first segment (tact) divided by the number of segments on a given side. The burst duration decreases along the body much like the trout-type. The delay between ends of activations however, equal zero ( $D_e = 0$ ), hence all activation on a given side ends at the same time. There is only activation on one side at a time for this case.

### **3. SUMMARY OF IMPORTANT BIOLOGICAL RELATIONSHIPS**

The following statements are meant to summarize some of the important relationships which have application in developing an undulatory system.

1. The time delay between activation of segments is always a fixed percentage of cycle time.
2. The speed of swimming is proportional to frequency of oscillation and speed of flexure wave propagation.
3. An increase in stiffness is required to increase frequency.
4. The left and right sides of individual segments are alternately activated.

## MYOTOME ACTIVATION PARAMETERS



T = CYCLE DURATION

t act = BURST DURATION

Dd = DELAY BETWEEN ACTIVATION OF MYOTOMES

De = DELAY BETWEEN ENDS OF ACTIVATION

Figure 3

5. The duration of excitation does not exceed 1/2 of cycle time.

6. Different muscle systems are used for slow and fast swimming.

7. Thrust is in the form of pulses at twice the frequency.

8. Distribution of amplitudes of undulation are directly correlated to basic structure. ie mass, cross section area, and areas of lateral projection.

#### **4. UNDULATORY SYSTEM EXPERIMENTS, RESULTS AND ANALYSIS**

##### **4.1 Shape Memory Alloy (SMA) muscle mechanism**

Shape Memory Alloy (SMA) technology and the "shape Memory Effect" is well described in the literature [references 27-42]. References can be found which date back several decades. The most extensively investigated material is the Nickel-Titanium alloy which is usually fabricated as 50% Nickel. Basically, the crystalline structure within the material can be cycled between two geometric states, namely martensite and austensite, by application and removal of heat. When this transition occurs a measurable shape change occurs in the material. In the martensite (cool) state the crystals are in an orthorhombic or elongated form and the material is relatively limber. When the material is heated above the austensite temperature threshold, the crystals switch to a cubic form which is much tighter and causes the material to contract very rapidly. This transition can be made to occur by the application of electrical pulses. This material then behaves much like an organic muscle fiber. Detailed comparisons of muscle with various types of artificial actuators including SMA mechanisms has been studied by Hunter and Lafontaine [16]. They incidentally have been of great assistance to us in developing a practical understanding of this technology. The power to mass ratio of a nickel-titanium (Nitinol) fiber is about 1000 times greater than muscle. This is without consideration of mass or volume of cooling system should this be required. A plot of the nominal (recommended recovery) force of various diameter wires (Flexinol) is plotted in Figure 4. This is about one third of the maximum recovery force and this value is used to preserve the factory training. The bias force is also plotted in the same figure. This is the force that should be applied to extend the wire as it cools. This value is typically about 5% to 10% of the maximum force.

The contraction time of an SMA wire depends on how fast one can heat the wire, hence is directly dependent on the risetime and amplitude of the current pulse. The relaxation time, however, is dependent on the time it takes to cool the wire (thermal diffusion).

##### **4.2 Single Segment Configuration**

FORCE VERSUS SMA WIRE SIZES  
VARIOUS SIZE FLEXINOL WIRE  
50 TO 250 MICRON DIAMETER

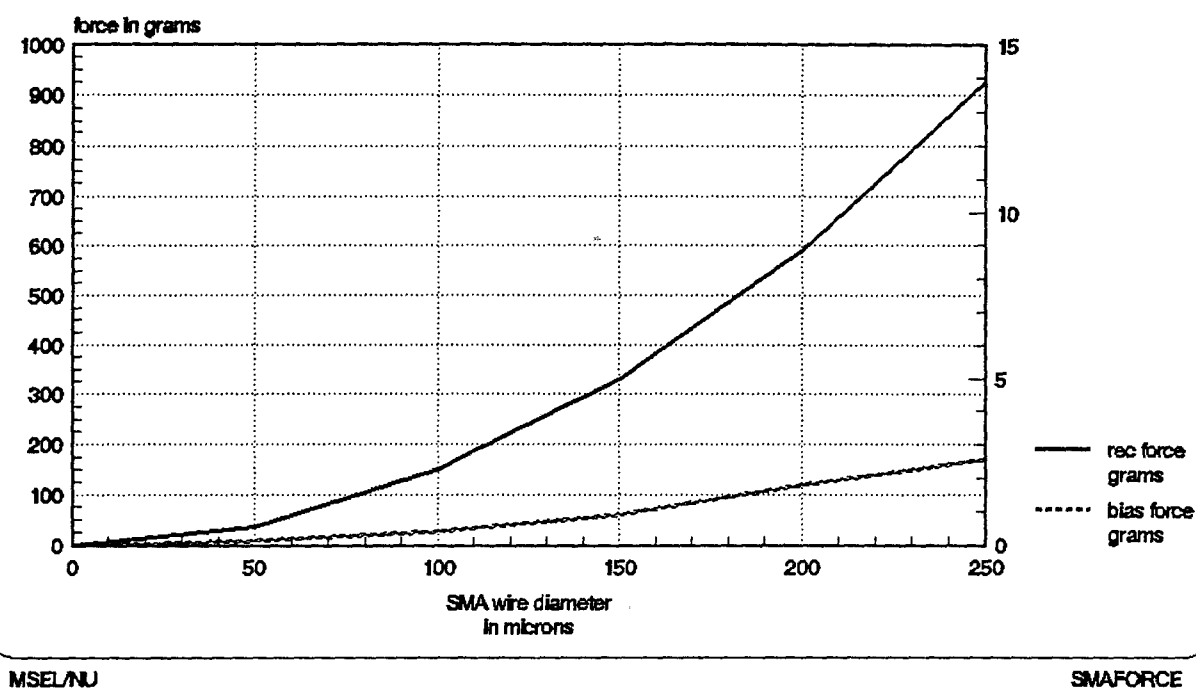


Figure 4

The basic system envisioned to demonstrate undulatory motion will of necessity include several segments. The material selected to serve as the notochord (backbone) of the skeletal system for this phase is a polyurethane material (1/8" x 1" x 4"). This material is flexible, and has various grades of stiffness, and has good temperature and water absorption properties. Specification for this material are included in Appendix A. We selected a material which has a stiffness measure which approximates the bias force of the nitinol wire thus eliminating the need to provide an external bias force. Figure 5a is a photo of a single segment used for initial experimentation. The vertebrae are made of teflon and each has 4 holes spaced 1/8" apart (from center) which serve as optional attachment points for the wires. The photo also shows tuners (harpsichord) which were used to adjust the initial SMA wire tension.

#### Contraction and Relaxation Speed

A series of experiments was conducted with the above single segment configuration prior to conducting experiments with a multi-segment configuration. A sensor was used to measure motion of the segment (perpendicular to the notochord axis), and it's output voltage versus deflection and contraction force required is shown in Figure 6. Experiments were carried out to assess contraction and relaxation times (hence cycle rate) both in air and in water at about 20 degrees C.

Experiments in air single segment Plots of contraction time and relaxation time versus peak current input in air is shown for 150 micron wire (70 degrees C wire) in figures 7. Note the pronounced decrease in contraction time as the current amplitude is increased (ie pulse width is decreased). For a fixed ampere-seconds product input, the total time for contraction and relaxation appears to be very nearly a constant. This constant essentially determines the maximum cycle rate for the wire under the existing ambient conditions.

Smaller diameter wire cools faster than the larger diameter wire. This is due to the larger surface to mass ratio for the smaller wire. For the 150 micron wire in air with a small cooling fan, the maximum cycle rate is about 1.1 seconds whereas it is about 0.7 seconds for the 100 micron wire. For a single segment having antagonistic wires on each side this implies a cycle rate of 2.2 seconds (0.45hz) and 1.4 seconds (0.7 hz) respectively for these two size wires. This is demonstrated in Figures 8a and 8b. Notice in these plots that a delay is required between alternate side activation to allow the wire to cool and begin to relax. This side to side activation delay is important and must be included when designing multiple segment coordination strategies as will be seen later.

Experiments in water single segment The same single segment system (100 micron wire) was immersed in de-ionized water at room temperature to measure the effects of liquid cooling on the

FIGURE 5A. SINGLE SEGMENT

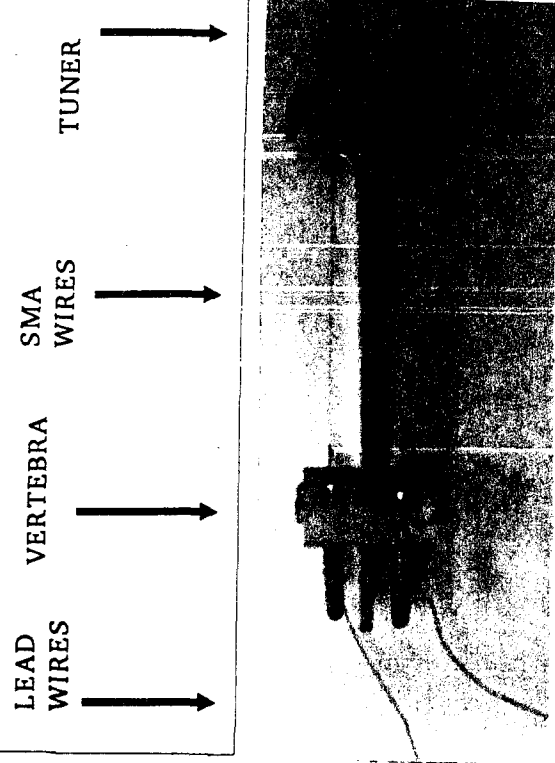


FIGURE 5C. 4 SEGMENT TEST CONFIGURATION

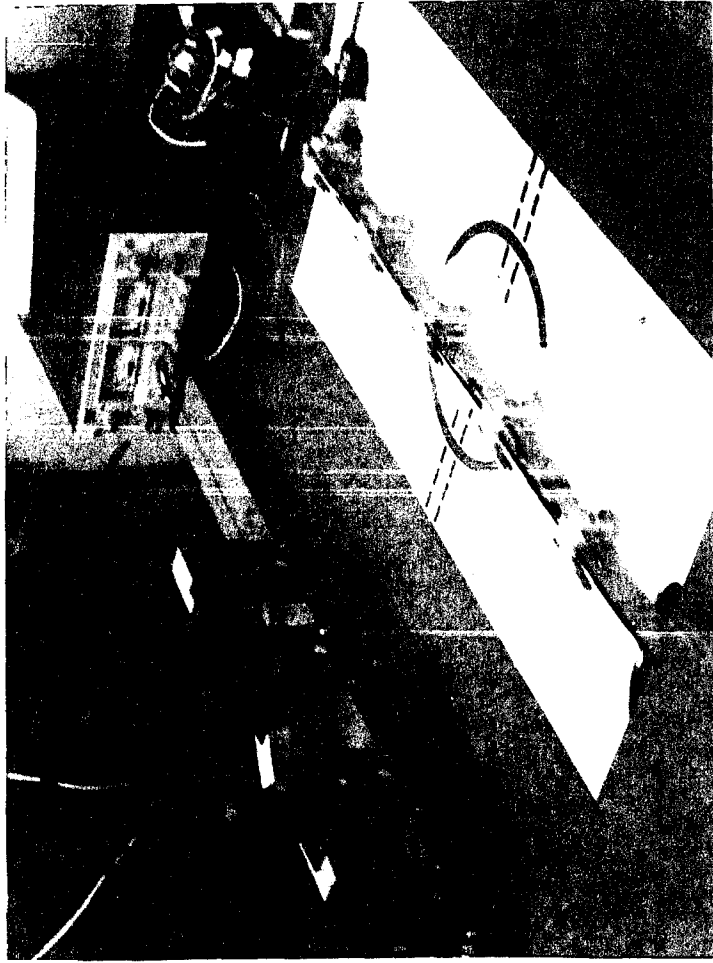
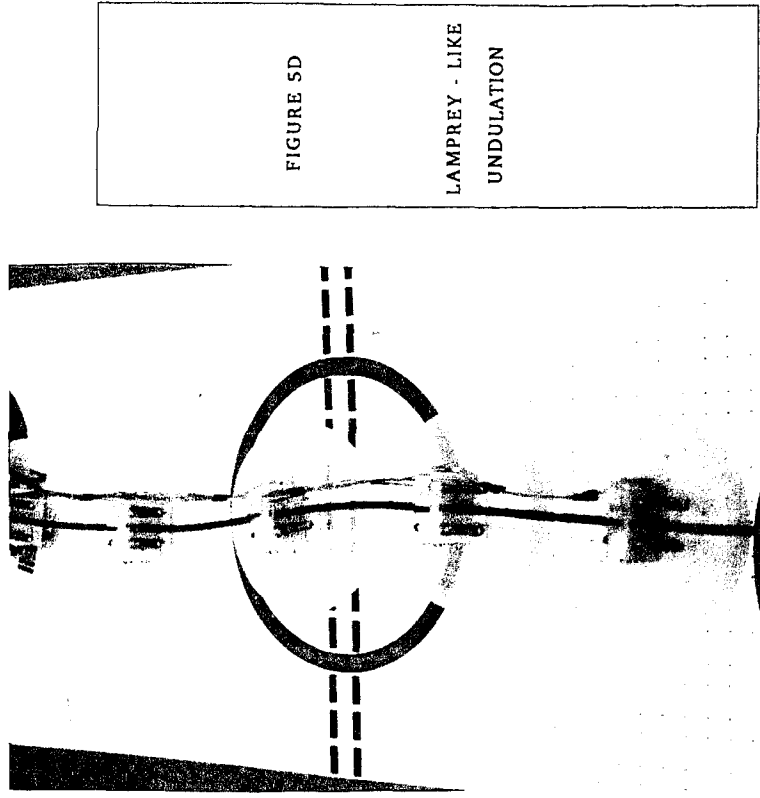


FIGURE 5B. 4 SEGMENT SKELETAL SYSTEM



FIGURE 5D

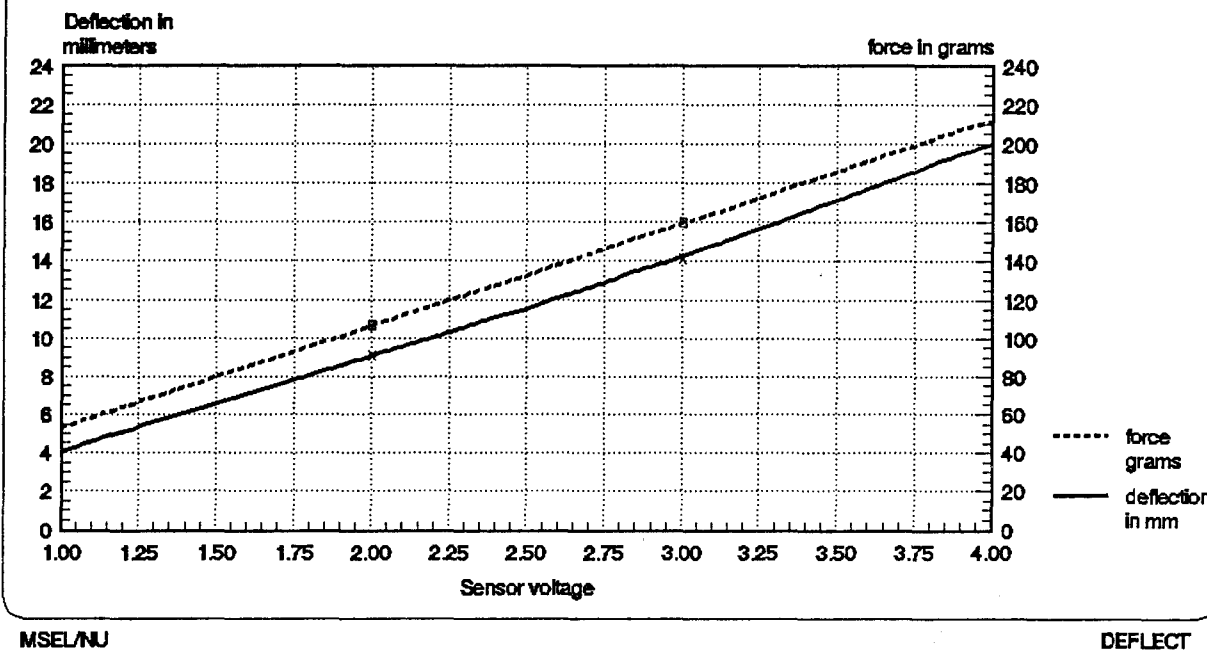


LAMPREY - LIKE  
UNDULATION

## DEFLECTION SENSOR & FORCE CALIBRATION

Polyurethane (85A) backbone segment

4 inch long x 1 inch x 1/8 inch  
(holes 2 and 3) 1/8 inch separation

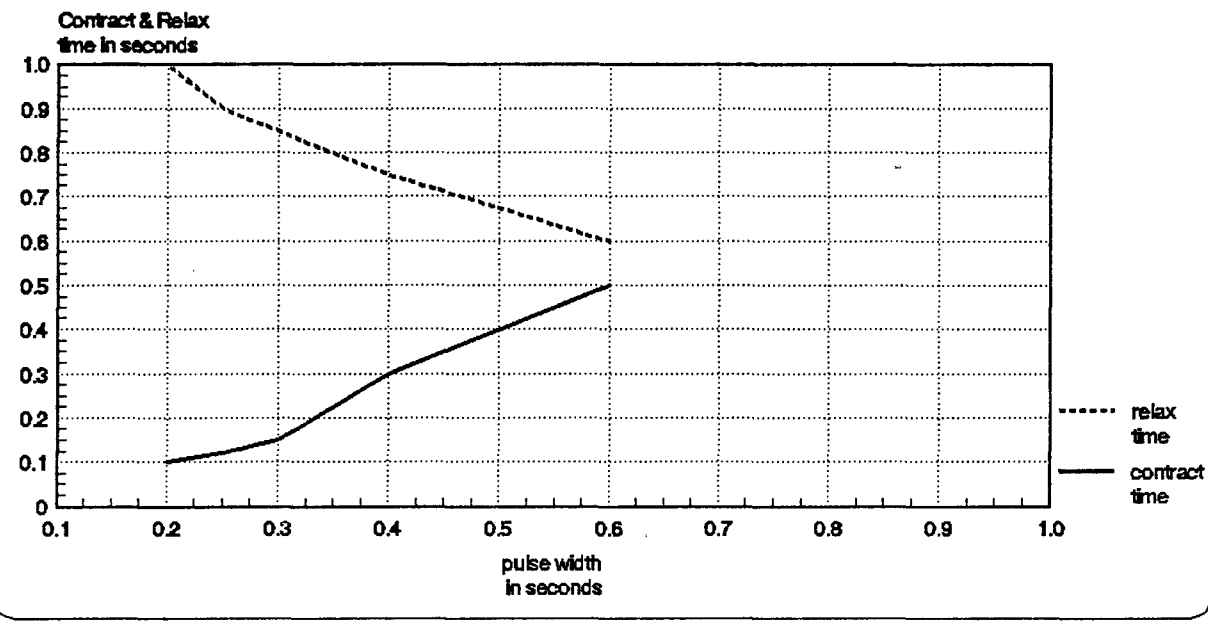


MSEL/NU

DEFLECT

Figure 6

**CONTRACTION AND RELAXATION TIMES IN AIR  
150 MICRON WIRE ONE SIDE OF SEGMENT  
CONSTANT VALUE OF AMP-SEC = 0.24  
FOR VARIOUS PULSE WIDTHS & AMPLITUDES**

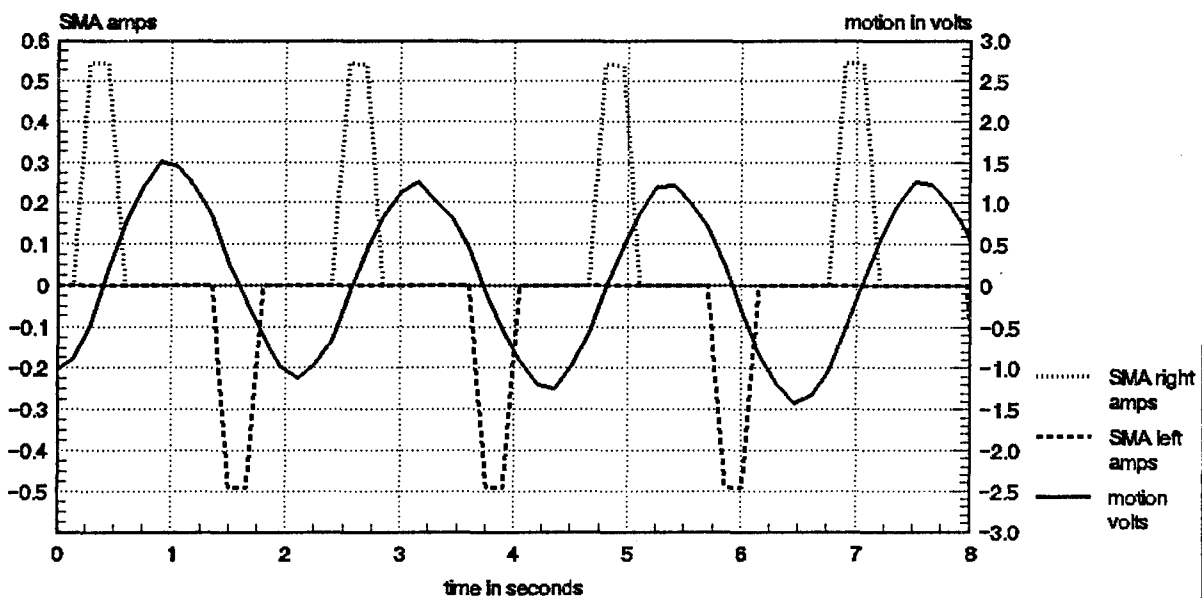


MSEL/NU

SPEED

Figure 7

**SMA MOTION VERSUS PULSE INPUT IN AIR**  
**SINGLE TWO SIDED SEGMENT**  
**150 MICRON WIRES**  
**.25 sec pulse @ 0.55 amps**

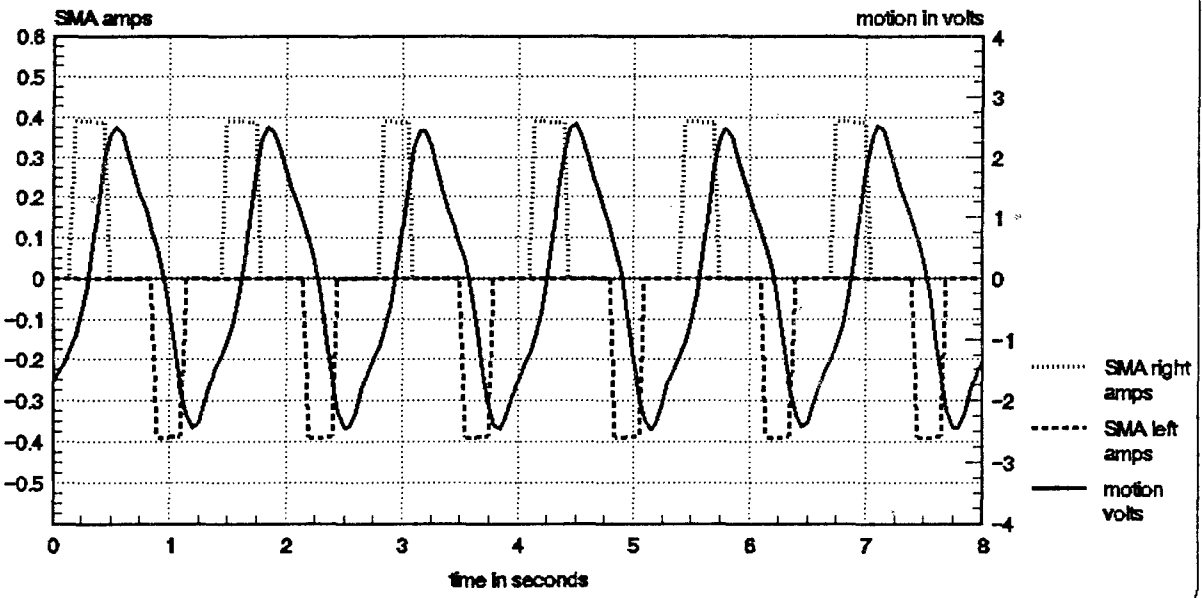


MSEL/NU

SEG1MAV2

Figure 8a

**SMA MOTION VERSUS PULSE INPUT IN AIR**  
**SINGLE TWO SIDED SEGMENT**  
**100 MICRON WIRES**  
**.3 sec pulse @ 0.4 amps**



MSEL/NU

SEG142AV

Figure 8b

relaxation time of the SMA wires and to measure the power required in this environment. The results show that the cycle rate for a single wire is about 0.13 seconds resulting in a cycle rate of 0.26 seconds for a two wire segment. Figure 9 is a plot of the drive current signals and the resulting oscillatory motion of a segment in water. The frequency of oscillation in water is about 4 hertz as compared to 0.7 hertz in air. For a single wire in water the average current requirement was 0.4 amps hence each wire is operating at a 0.4 amp-hr rate at 4 hertz operating frequency. For a 4 segment undulatory system in 20 degree C water, this would amount to a 3.2 amp-hr rate at 18 volts.

SMA current amplitude in water In Figure 10 we have plotted the SMA current amplitude at a fixed pulse width (pulse width = 63 msec) versus notochord deflection. This data was acquired during the in water experiments. The data shows that segment deflection or motion is proportional to the amplitude of the applied current. This is significant in terms of controlling the amplitude of oscillation of a multi-segment undulatory system as will be seen later.

#### 4.3 Four Segment Undulatory System Experiments

##### 4.3.1 Mechanical configuration

A simple skeletal system was designed and constructed for the purpose of conducting experiments aimed at demonstrating undulatory motion. It was determined that by making use of a continuously flexible backbone system that fewer SMA actuators would be required to show smooth undulatory behavior. As mentioned earlier the backbone material is polyurethane (Durometer 85A) manufactured by Harkness Industries (Appendix A). Photos of the skeletal system and test configuration are shown in Figures 5b and 5c. The total length of the backbone is 2 feet long, and it is 1 inch high, and 1/8 inch thick. It has 5 solid teflon vertebrae located 4 inches apart. They serve as attachment points for the SMA wires and for tuners which are used to adjust initial wire tension. The configuration uses single 3 inch SMA wires (100 micron diameter) on each side of each segment for a total of 8 wires.

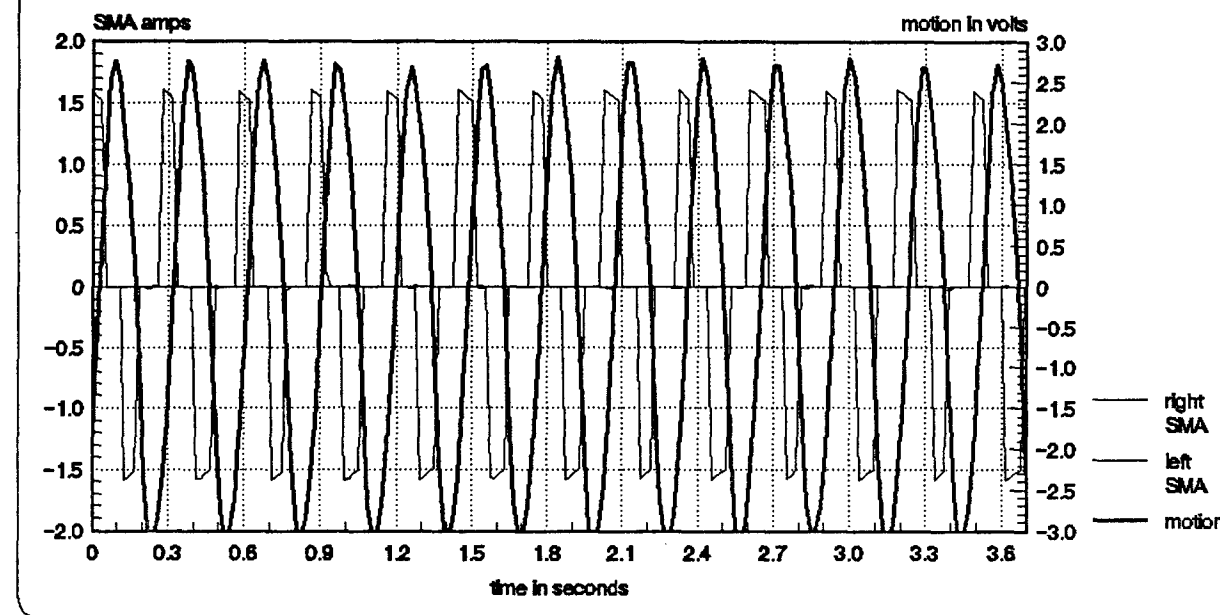
##### 4.3.2 Neural control system

Typical neural control signal timing which governs muscle actuation of Lampreys or Eels are depicted in Figure 11 for a 4 segment system. The upper (positive) traces depict left side activation while the lower (negative) traces depict right side activation. The center traces depict those closest to the head and the farthest from the center those closest to the tail. The delay is represented as the time between activation of successive segments on a given side and the body flexure wave activation frequency is determined by the cycle time of the first segment.

A circuit was designed and fabricated to generate the necessary signals and to drive the SMA wires. The circuit allows for

**SMA MOTION VERSUS PULSE INPUT IN WATER  
SINGLE TWO SIDED SEGMENT**

100 MICRON WIRES  
63 msec pulse @ 1.6 amps

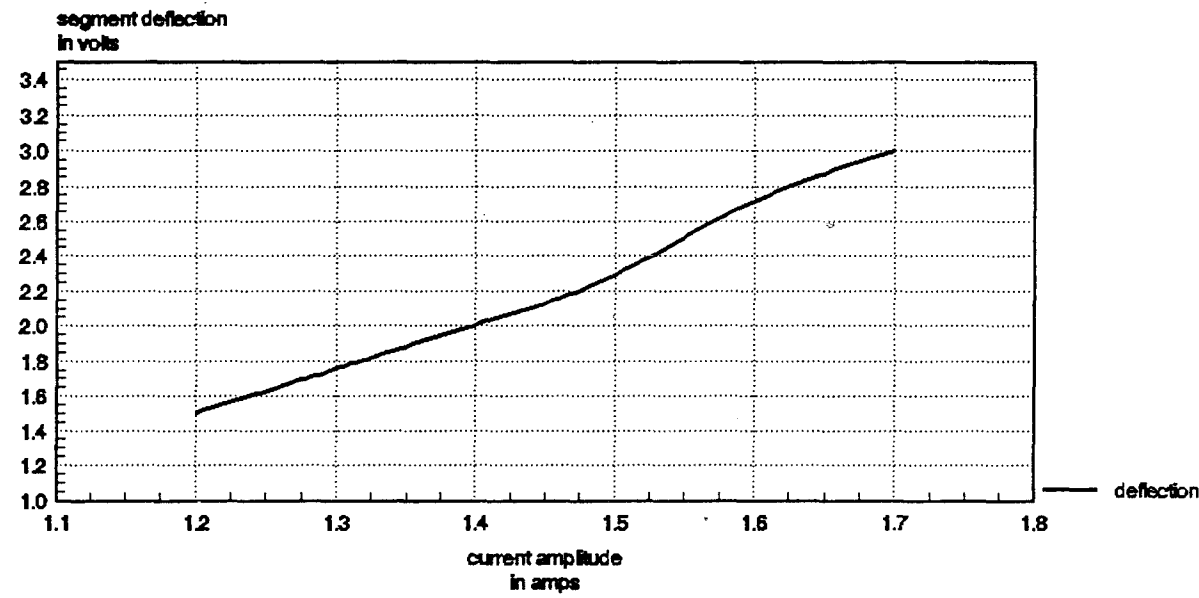


MSEL/NU

Figure 9

WAT2W19

**SEGMENT DEFLECTION VERSUS SMA INPUT  
CURRENT AMPLITUDE @ PULSE WIDTH = 63msec  
IN WATER TEST DATA  
100 MICRON WIRES**

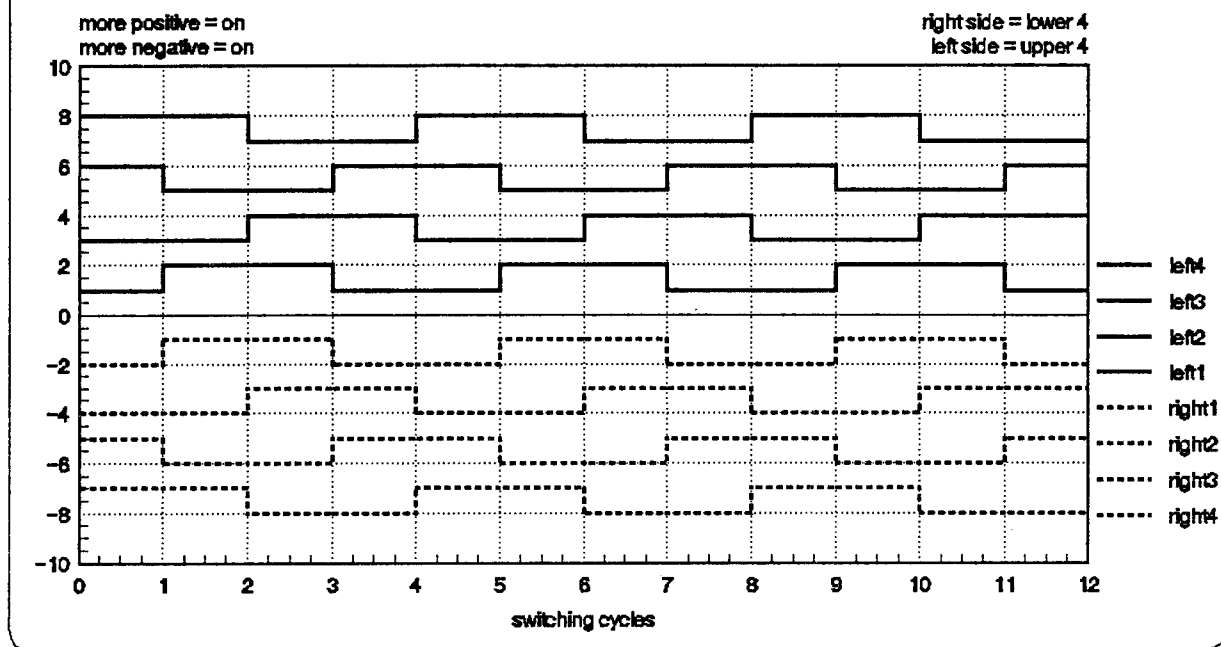


MSEL/NU

Figure 10

IVSDEF

**GENERAL TIMING DIAGRAM - LAMPREY  
FOUR SEGMENT MODEL W/8 ACTUATORS  
FOUR ON LEFT SIDE AND FOUR ON RIGHT SIDE**

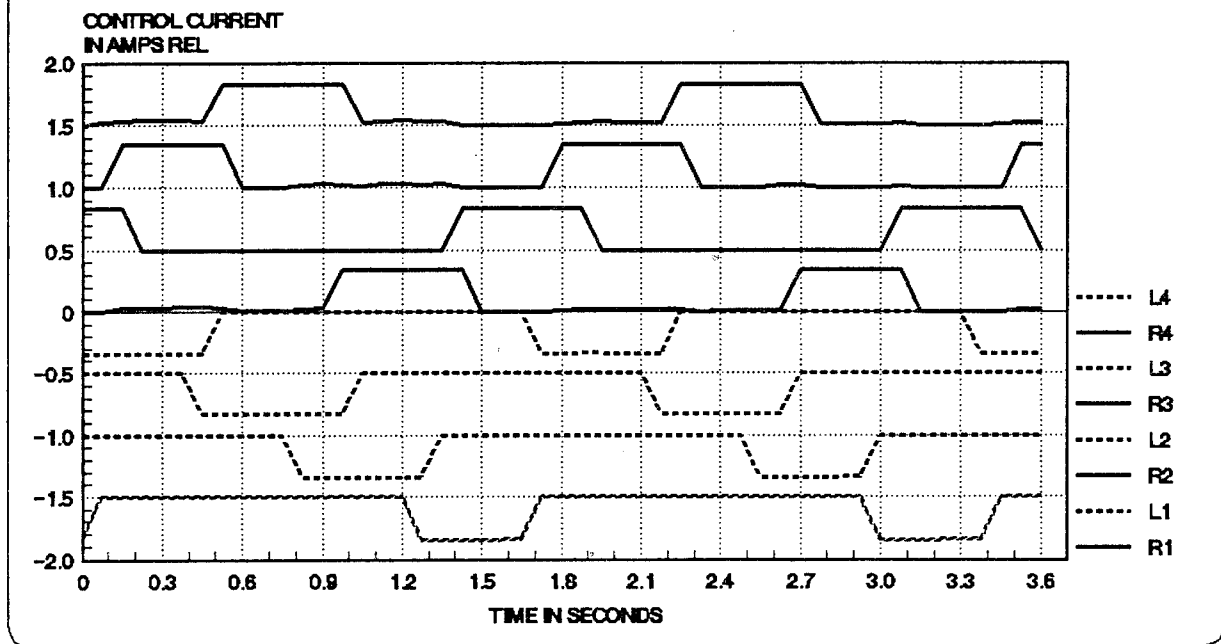


MSEL/NU

Figure 11

TIMING1A

**LAMPREY CONTROL CURRENT  
FOR 4 SEGMENT SYSTEM  
PHASE DELAY = 0.75 \* PW**



MSEL/NU

Figure 12

AIR75LMP

changing the each of the pulse widths (duration), pulse frequency (cycle time), intersegment phase delays, and signal amplitude. These signals will later be generated and controlled by a small microprocessor. Figure 12 depicts the actual control signals generated by the circuit. Notice that there is a built in delay between activation of antagonistic sides of an individual segment. This is required to allow for the SMA wire's finite relaxation time (cooling time) prior to activating the opposite side.

#### 4.3.3 Experimental Setup and Data Acquisition System

The experimental system setup is shown in Figure 5c. The undulatory system was placed on an air table to minimize friction drag due to gravity. Four ultrasound sensors were used to track the motion of each of the four vertebrae during operation. The ultrasound sensor frequency was 215 kHz and the output is a continuous analog output voltage proportional to distance from the transducer head. These sensors were operated at 100 hertz sampling rate.

The components of the data acquisition system included a DT-2801A Data Translation board which was mounted in a laboratory PC. It provides for sixteen 12 bit A/D channels with a 27.5 kHz throughput and selectable gain. It also has two 12 bit D/A outputs and two 8 line digital I/O ports and a programmable clock. The system was programmed to sample the voltage across each of the 8 SMA actuators as well as the output from the four transducers. The data were then plotted and printed from a PC using a graphical plotting program.

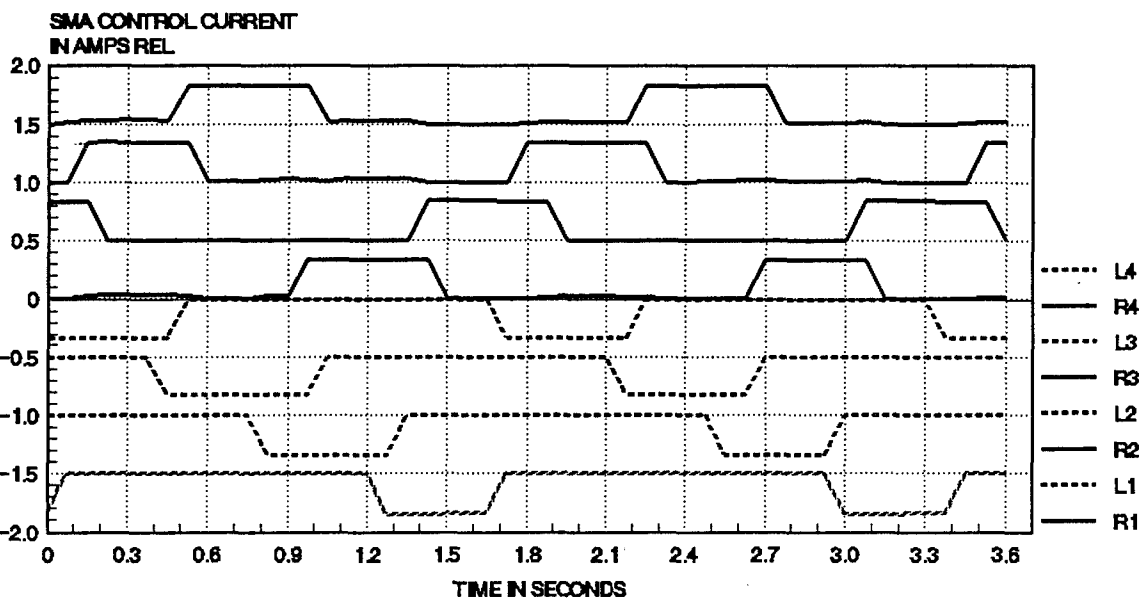
An 8mm video camera and recorder were used to document and further analyze the motion resulting from a variety of neural control configurations. Additionally, a VHS video camera was used to document various experiments. A 6 minute narrated video was produced depicting the results of this phase of the project.

#### 4.3.4 Experimental results - four segment undulator

We investigated four types of coordination which correspond to the four types of synergies described earlier for steady swimming of different fish.

The first type of coordination is similar to that of a Lamprey or Eel. The control signals and the resulting vertebral motion is depicted in Figure 13a, and 13b respectively. The pulses in each segment are the same width, and the activation delay is equal to the deactivation delay. The phase delay in this configuration is 3/4 (0.75) of the pulse width (PW) (see calculations in appendix C). In this configuration, the first segment of the left side is activated at about the same time as the third segment on the right side. The nominal amplitude of the current pulses in each wire is about 0.35 amps and the cycle time is 1.7 seconds. The oscillatory motion of the vertebrae is quite smooth and the progression of the motion (wave) from the first segment (MOVE1) to the fourth (MOVE4) is obvious. One can also see the

**LAMPREY CONTROL CURRENT  
FOR 4 SEGMENT SYSTEM**  
**PHASE DELAY = 0.75 \* PW**  
**AIR TABLE DATA**

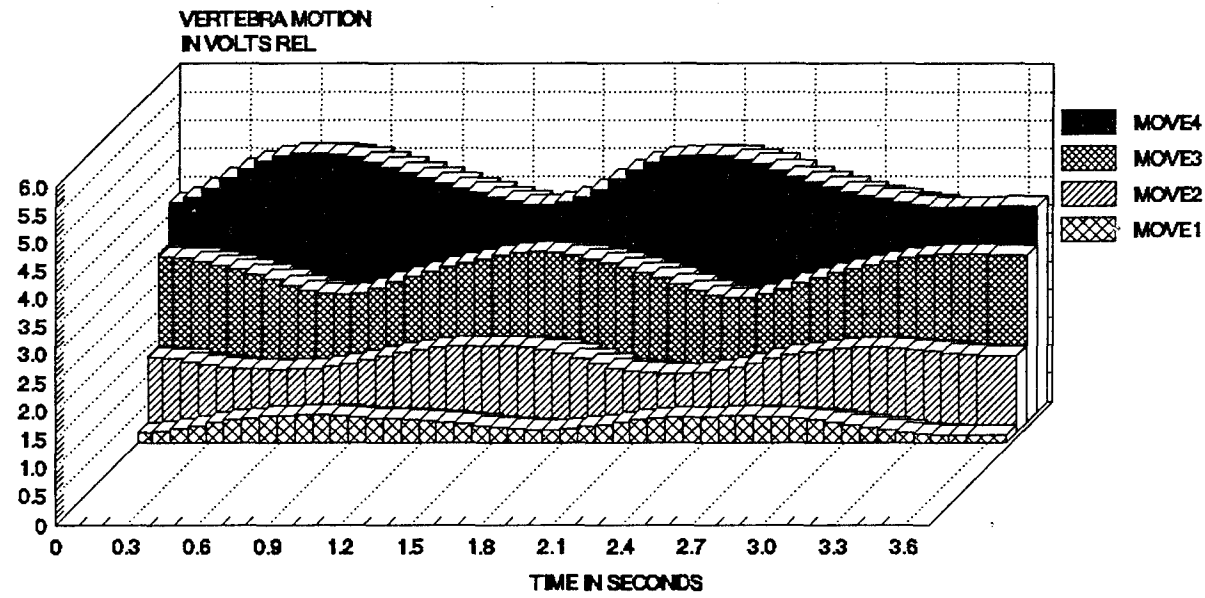


MSEL/NU

AIR75LMP

Figure 13a

**LAMPREY RELATIVE MOTION  
AT VERTEBRAE – FOR 4 SEGMENT SYSTEM**  
**PHASE DELAY = 0.75 \* PW**  
**AIR TABLE DATA**



MSEL/NU

AIR7LMPB

Figure 13b

resultant motion in the photo of Figure 5d.

The second coordination type (Carp) involved reducing the phase delay between segments. All other parameters (pulse width, side to side delay, and current amplitude) remained essentially the same as in the first type. Figure 14a and 14b show the control signals and the resultant vertebral motion of the system. This type of coordination leads to having a larger percentage of body length activation with time on a given side and results in a larger amplitude motion at the tail (fourth segment) of the system.

The third type (Trout) of coordination is a much like a combination of types one and four. The phase delay is  $3/4$  of the pulse width of the first segment but the activation pulse widths decrease along the body. There is, however, side to side overlap of activation (unlike the shark). The resultant motion is oscillatory (Figures 15a, 15b).

The fourth coordination configuration is similar to that of a shark. Figures 16a and 16b depict the control signals and resultant vertebral motion response. The phase delay in this configuration is one fourth ( $0.25 \times PW$ ) of the first segment's pulse width. The basic cycle time (1.7 seconds) is the same as all cases described above. Notice that each successive pulse width is decreased along one side of the body and that there is no side to side overlap of activation. Also notice that the activation of all segments on a given side terminate simultaneously. The result is that an undulatory wave is not discernible. The motion as seen on the video is more like a side to side whipping action.

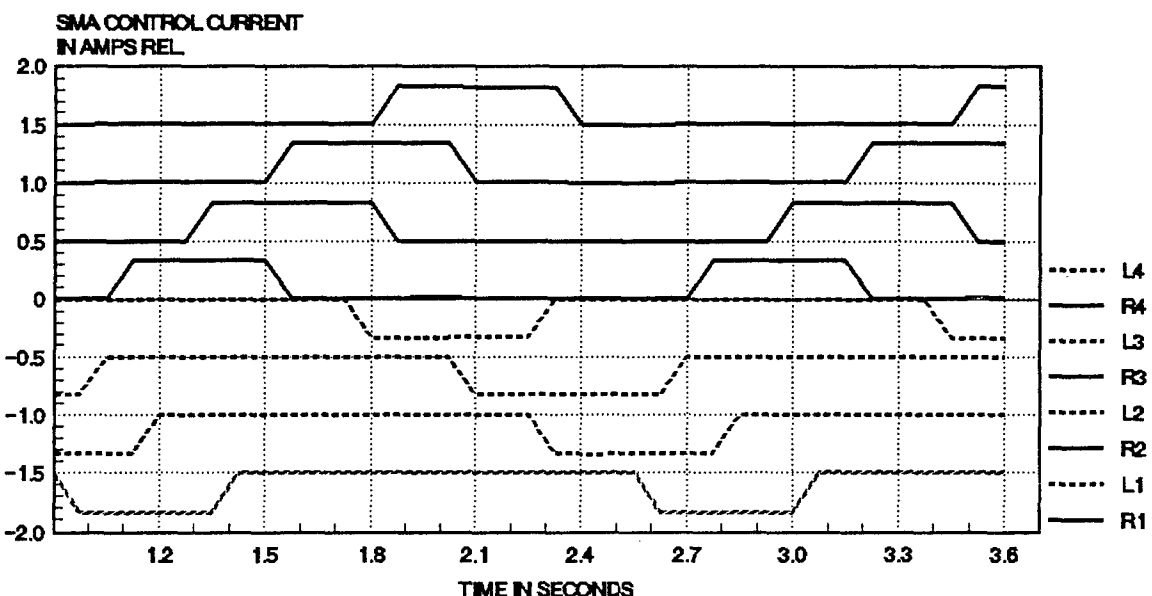
#### 4.3.5 Discussion

The above experiments were carried out using a skeletal system. The system body mass and its relative distribution, to simulate specific types of fish, were not incorporated in this phase hence the resultant motion does not exactly replicate that of specific coordination types. The Lamprey or Eel response, however, is a closer approximation since their mass is more equally distributed than the other types (Figures 1a and 1b).

The experiments carried out on the 4 segment system above were all conducted in air. Based on our single segment experiments in water as described earlier, it appears that the cycle time of the 4 segment system could be reduced from 1.7 seconds to about 0.25 seconds (4 hertz). This is close to an order of magnitude improvement in flexion wave frequency due to the faster cooling time in room temperature water. This oscillatory response frequency coincides with nominal frequencies of fish this size.

The tradeoffs for developing undulatory systems similar to that described here are: (1) Improvement in frequency of undulation for a given wire size can be achieved by immersion in a liquid bath, however at a cost of increased SMA power require-

**CARP-LIKE CONTROL CURRENT  
FOR 4 SEGMENT SYSTEM**  
**PHASE DELAY = 0.5 $\times$ PW**  
**AIR TABLE DATA**

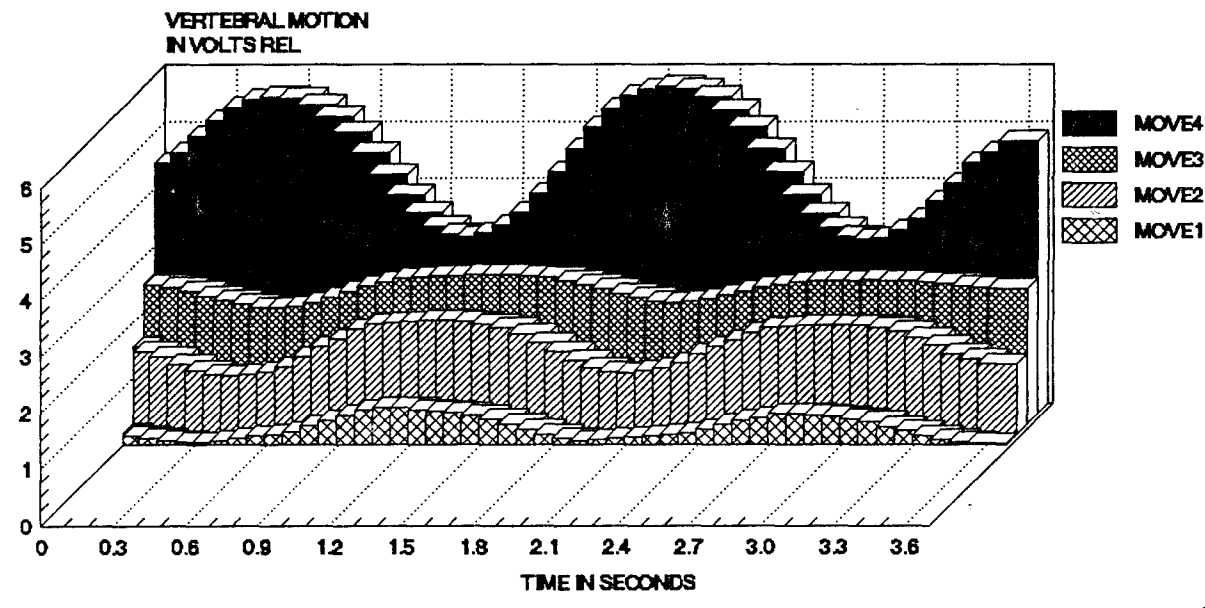


MSEL/NU

AIRSLM5B

Figure 14a

**CARP-LIKE RELATIVE MOTION  
AT VERTEBRAE – FOR 4 SEGMENT SYSTEM**  
**PHASE DELAY = 0.5 $\times$ PW**  
**AIR TABLE DATA**

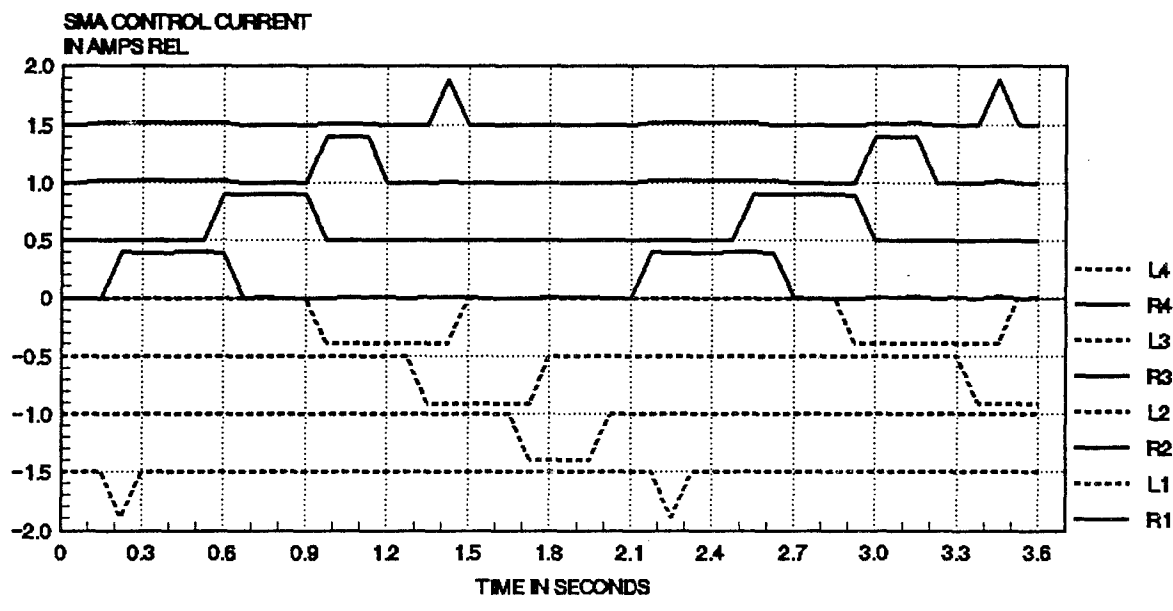


MSEL/NU

AIRSLM5D

Figure 14b

**TROUT-LIKE CONTROL CURRENT  
FOR 4 SEGMENT SYSTEM**  
**PHASE DELAY = 0.75  $\mu$ PW**  
**AIR TABLE DATA**

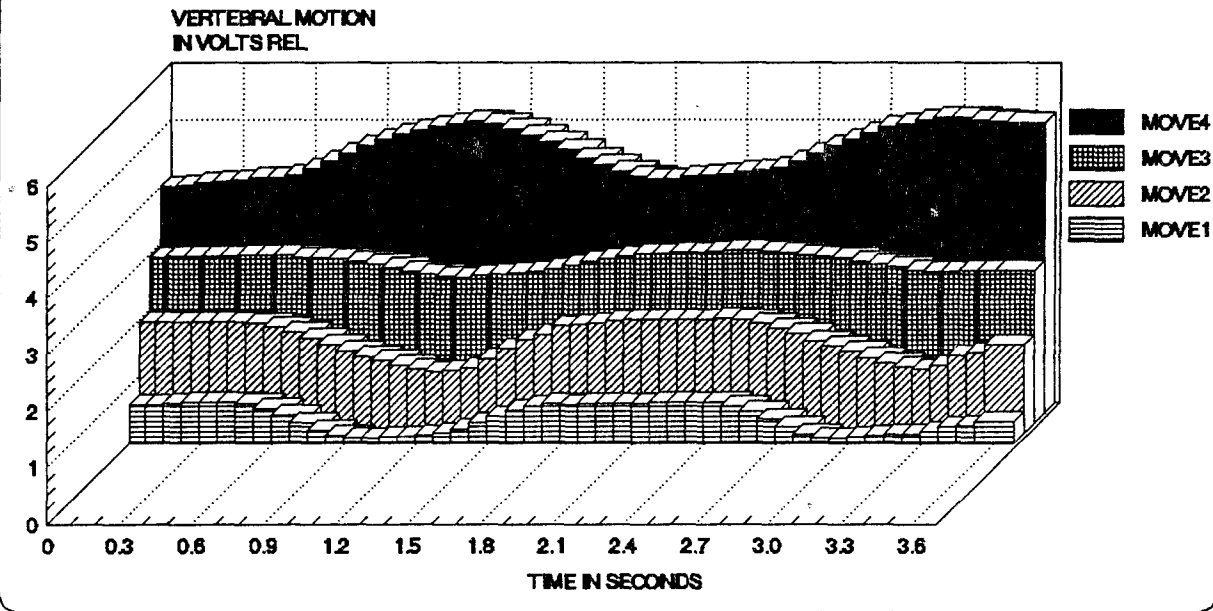


MSEL/NJ

TROUTR1

Figure 15a

**TROUT-LIKE RELATIVE MOTION  
AT VERTEBRAE - 4 SEGMENT SYSTEM**  
**PHASE DELAY = 0.75  $\mu$ PW**  
**AIR TABLE DATA**

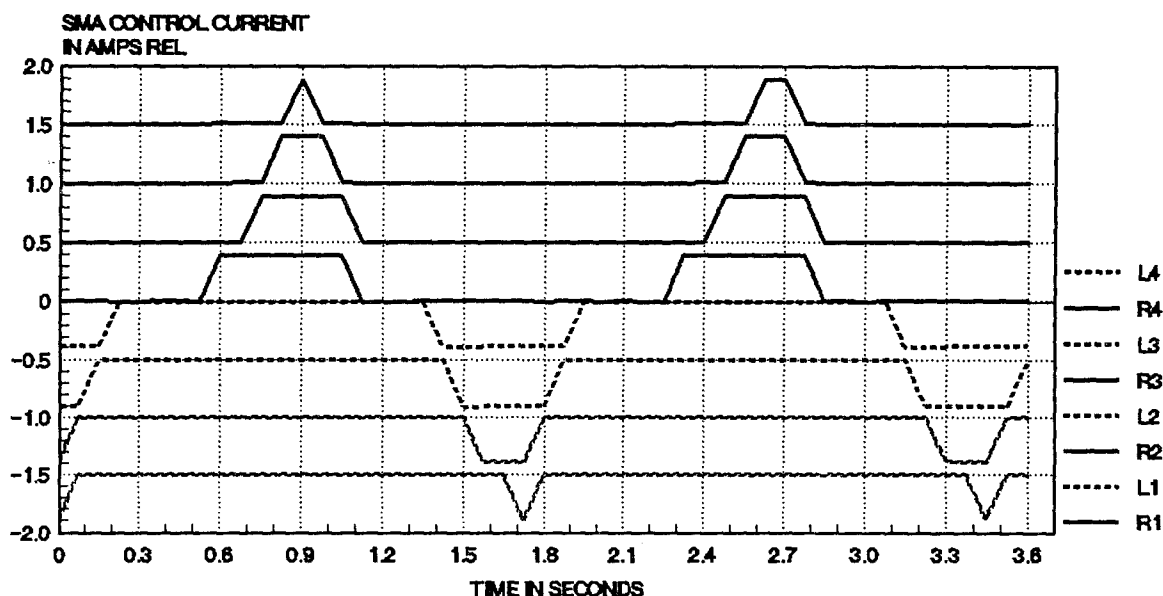


MSEL/NJ

TROUTR1B

Figure 15b

**SHARK-LIKE CONTROL CURRENT  
FOR 4 SEGMENT SYSTEM**  
PHASE DELAY = 0.25·PW  
AIR TABLE DATA

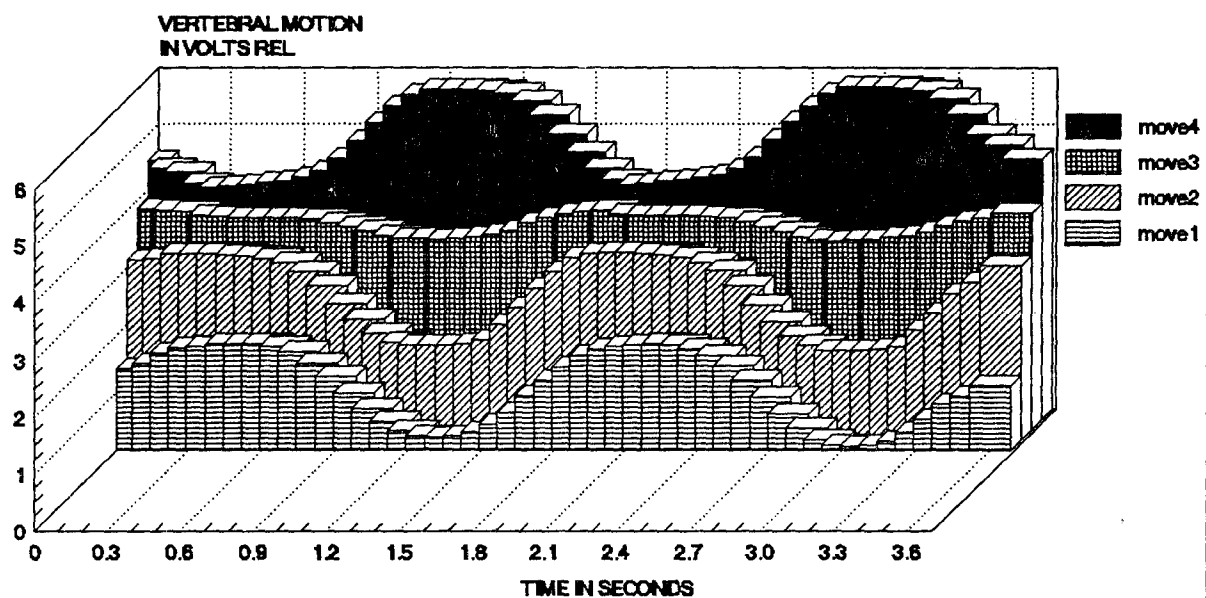


MSEL/NU

SHARKR4

Figure 16a

**SHARK-LIKE RELATIVE MOTION  
AT VERTEBRAE - 4 SEGMENT SYSTEM**  
PHASE DELAY = 0.25·PW  
AIR TABLE DATA



MSEL/NU

SHARKR4B

Figure 16b

ments. (2) The minimum size wire which can provide the required force will have the fastest response time. (3) If the contraction is maintained to about 3 percent, the wires can withstand hundreds of thousands of cycles of operation.

We ran a brief life cycle test of an SMA wire attached to a single segment system. The wire ran over 110, 000 cycles and was still operable. Further life cycle testing will be conducted during the next phase.

We have been experimenting with using type K (Nickel-Chromium vs. Nickel-Aluminum) thermocouples (at the suggestion of Ian Hunter and Serge Lafontaine) to measure SMA wire temperature under transient conditions. This could prove to be an excellent feedback mechanism for undulation control. We can measure temperature change in the wire with applied current, however, the thermocouple as tested was influenced by ambient conditions. We will be further investigating means of insulating the thermocouple from the environment as well as acquiring data on temperature versus time profiles relative to current input for various ambient environments.

##### **5. SUMMARY OF RESULTS AND CONCLUSIONS**

A skeletal system was developed to investigate fish like swimming characteristics. It provided for segmentation of a body and for propagation of waves of flexure along the body. The system consisted of 4 segments and a total length of 20 inches.

The system was used to demonstrate frequencies of 0.7 hertz in air and a potential for 4 hertz in 20 degree C water. The latter is similar to frequencies encountered in swimming fish of comparable size.

A polyurethane material was used to imitate a fish notochord and served to provide a restoring (bias) force for the muscle wires.

Shape memory alloy wires of 100 micron diameter were used as muscles. They produce about 3% contraction when pulses of current were applied. The contraction speed and developed force is related to the risetime, amplitude, and duration (which causes heating of the SMA wires) of the current pulse input. The restoration (relaxation) to original length is assisted by the elastic force of the polyurethane notochord.

Each segment consisted of left and right shape memory alloy "muscles" attached to solid teflon vertebrae. Each wire was initially tuned by hand using harpsichord tuners. The left and right wires were made to contract alternately in counterphase.

Coordination of segments was controlled by an electronic module. Four types of synergies were evaluated. They differ in terms of phase delay between segment activation, deactivation, and activation pulse width. The coordination types were selected

to agree with those developed from experiments with intact fishes.

This phase of the project demonstrated very clearly that the basic mechanisms for generating undulatory motion similar to that of fish in small robotic systems are realizable.

## Biological References

- [1] Ayers, J., Carpenter, G., Currie, S. and Kinch, J. "Quantitative Analysis of Normal and Regenerating Behaviors in the Sea Lamprey", Soc. Neurosci. 6, 466, (1980).
- [2] Ayers, J., Carpenter, G., Currie, S. and Kinch, J., "Which Behavior Does the Lamprey Central Motor program Mediate?", Science 221: 1312-1314 (1983).
- [3] Ayers, J., "Recovery of Oscillator Function Following Spinal regeneration in the Sea Lamprey". In: Cellular and Neuronal Oscillators. J. Jacklet, [ed]. Marcel Dekker, New York, Pp. 349-383 (1989).
- [4] Aleev Y.G. 1963. Function and gross morphology in fish. Jeruslem: Israel Prog. Scientific Trans.
- [5] Alexander R.M. 1967. Functional design in fishes. London: Hutchinson Lib. 160 pp.
- [6] Azuma Akira. 1992. The Biokinetics of Flying and Swimming.
- [7] Bainbridge R. 1958. The speed of swimming of fish as related to size and the frequency and amplitude of the tail beat. J Exp. Biol. 35: 109)133.
- [8] Bainbridge R. 1961. Problems of fish locomotion: Vertebrate locomotion. Symp. Zool. Soc. [Lond} 5, 13)32.
- [9] Bainbridge R. 1963. Caudal fin and body movents in the propulsion of some fish. J Exp. Biol. 40, 23)56.
- [10] Blake R.W. 1983. Median and paired fin propulsion. In Fish Biomechanics (ed. P.W. Webb and D. Weihs), pp. 214-247. New York: Praeger Publishers.
- [11] Blake R.W. 1983. Fish locomotion Cambridge University Press, Cambridge.
- [12] Bone Q. 1966. On the function of the two types of myotomal muscle fibre in elasmobranch fish. Fish. J. Mar. Biol. Assoc. U.K. 46: 321-349.
- [13] ray, J. 1968. Animal Locomotion. Weidenfeld and Nicolson, London.
- [14] Grillner, Sten, and S. Kashin, "On the Generation and Performance of Swimming in Fish", Neural Control of Locomotion, Vol. 18, Plenum Press, 1976.
- [15] Grillner, Sten, and P. Wallen, "How Does the Lamprey Central Nervous System Make the Lamprey Swim", J. exp. Biol. 112, 337-357 (1984).

[16] Hunter, Ian W., and S. Lafontaine, "A Comparison of Muscle with Artificial Actuators", IEEE Sensors and Actuators, 1992.

[17] Kashin, S., A. Feldman, G. Orlovsky. 1979. Different forms of swimming in the carp, (*Cyprinus carpio* L. J. Fish Biol., 14, 403-406.

[18] Kashin, S., V. Smolianinov. 1978. Locomotion in water. In: *Lokomotsia zhyvotnykh i biomechanika oporno-dvigatelnogo appara-ta*. Kiev (in Russian).

[19] Kashin S., G. Orlovsky, A. Feldman. 1974 Locomotion of fish evoked by electric stimulation of the brain. Brain Res., vol. 82, 47-63.

[20] Lieber, R., R. Raab, S. Kashin, R. Edgerton. 1992 Sarcomere length changes during fish swimming. J. Exp. Biol. 169, 251-254.

[21] McClellan, Andrew D., "Control of Locomotion in a Lower Vertebrate, the Lamprey, Brainstem Command Systems and Spinal Cord Regeneration", Amer. Zool., 29:37-51(1989)

[22] Rovainen, Carl M., "Neurobiology of Lampreys", Physiological Reviews, Vol 59, No 4, October 1979.

[23] Sigvardt, Karen Ann, "Spinal mechanisms in the Control of Lamprey Swimming", Amer. Zool., 29:19-35(1989)

[24] Webb P.W. 1975. Hydrodynamics and energetics of fish propulsion. Bull. Fish. Res. Bd Can. 190: 1-158.

[25] Webb P.W. 1988. Simple physical principles and vertebrate aquatic locomotion. Am. Zool. 28: 709-725.

[26] Weihs, Daniel, "Design Features and Mechanics of Axial Locomotion in Fish", Amer. Zool., 29:151-160(1989).

#### **Engineering References**

[27] Beauchamp, C. et al, "Cambered Flexible Control Fins", NUWC, Newport RI., Symposium Flow Noise Modeling, Measurement, and Control, American Society of ME, Winter Meeting Nov-Dec 1993, New Orleans, La.

[28] Boggs, Robert N., "How Shape Memory Metals Shape Product Designs", Design News, June 1993

[29] Duerig, T.W., and K.n. Melton, "Designing With The Shape Memory Effect", Raychem Corp, MRS Int'l. Mtg. on Adv Mats. Vol 9, 1989 Materials Research Society.

[30] Dynalloy, Inc. "Technical Characteristics of Flexinol", Irvine, Ca. received 3 June 1994.

[31] Gilbertson, Roger, "Motorless Motion, Working with Shape

Memory Wires", Mondo-tronics, 1992.

[32] Hodgson, Darel E., "Using Shape Memory Alloys", Shape Memory Applications Inc., 1988

[33] Hodgson, Darel E., "Shape Memory Applications, Inc. brochure on materials and services.

[34] Iovine, John, "Experimenting With Shape Memory Alloys", Popular Electronics, June 1993.

[35] McLean, B.J., et al, "A Compliant Wing Section for Adaptive Control Surfaces", Martin Marietta, Denver Co., Paper presented at the SPIE Conf. on Active Materials and Adaptive Structures. Session 16, 1992.

[36] McLean, B.J., et al, "Modeling of a Shape Memory Integrated Actuator for Vibration Control of Large Space Structures", Martin Marietta Space Systems from Proceedings of US Japan Workshop on Smart/Intelligent Materials and Systems March 1990, Honolulu, Hawaii.

[37] McLean, B.J., et al, "Development of a Shape memory Material Actuator for Adaptive Truss Applications", MM Same conference.

[38] Nadolink, R. and C. Beauchamp, "Shape Memory Alloy Articulated (SMAART) Control Surfaces", NUWC, Newport RI, no date. received from Charlie Beauchamp.

[39] Nadolink, R. and C. Beauchamp, "Shape Memory Alloy Adjustable Camber (SMAAC) Control Surfaces", NUWC, Newport RI, no date. received from Charlie Beauchamp.

[40] Ostman, Charles, "Shape Changing Metals", Emerging Technology, Sep-Oct 1992

[41] Studt, Tim "Smart Materials: Creating Systems that React", R&D Magazine, April 1992

[42] TINI Alloy Company, "Introduction to Shape Memory Alloys" San Leandro Ca. Services, properties, catalog, components, and prices, June 1994.

[43] Cadillac Plastics, Information and specifications on urethane products, Londonderry, NH.

[44] GE Plastics, Information on Lexan products, Pittsfield Ma.

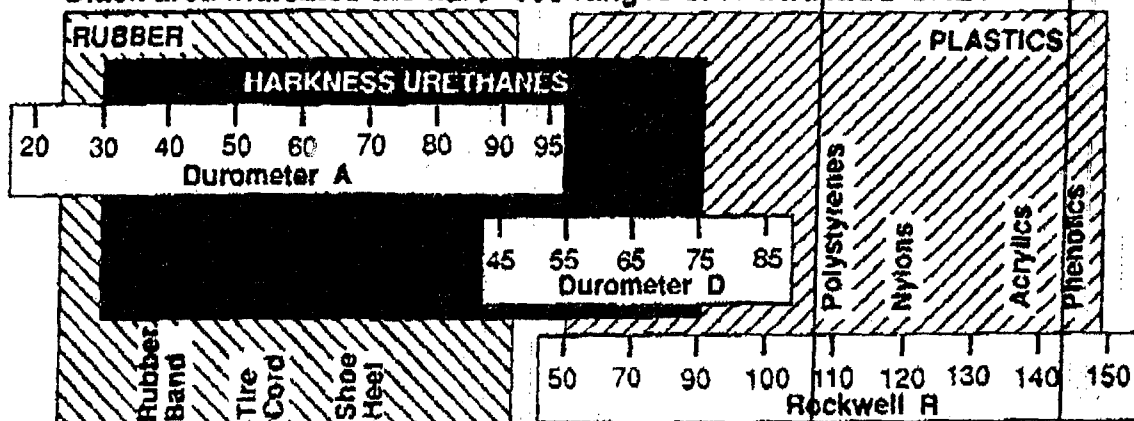
[45] Marshall, Joseph, Papers from DCC Corporation, "Hotspot" portable thermocouple welder, "Make your own Thermocouples", "Hotmux temperature Data Logger", and price list, June 1994.

## **Appendix A**

### **POLYURETHANE DATA SHEETS**

# HARKNESS Industries, Inc.

Black area indicates the hardness ranges of HARKNESS URETHANES



## URETHANE PRODUCT GUIDE

MECHANICAL PROPERTY	ASTM	MP300	MP600	MP750	MP850	MP900	MP950	MP160	MP175
Tensile Properties	Test								
Break, psi	D-412	380	4500	5500	6000	4500	5500	6500	7500
100% modulus, psi	D-412	80	250	350	600	1100	1800	3000	5500
300% modulus, psi	D-412	170	600	1000	1500	2100	4000	6500	-
Elongation, %	D-412	515	500	500	500	450	320	300	225
Break Set, %	D-412	-	5	10	10	10	10	15	-
Modulus of Elasticity, psi	D-638	-	500	1500	2500	5000	9000	12500	-
Compression Properties (Shape factor 0.56)									
Deflection, psi @ 5%	D-575	15	30	70	180	310	450	-	-
Deflection, psi @ 10%	D-575	25	70	140	390	625	890	-	-
Deflection, psi @ 15%	D-575	34	110	220	560	875	1170	-	-
Deflection, psi @ 20%	D-575	38	160	280	690	1125	1400	-	-
Deflection, psi @ 25%	D-575	44	220	330	800	1350	1600	-	-
Compression Set, %									
Method A @ 70° C	D-395	-	10	8	5	-	1	10	15
Method B @ 70° C	D-395	9	10	15	25	30	40	50	-
Durometer, Shore ± 5	D-2240	30A	60A	75A	85A	90A	95A	60D	75D
Tear Properties, pli, Die C	D-624	90	200	250	400	400	450	700	850
Abrasion Resistance, Tabor									
H10 @ 1000gm. load, mg. loss per 1000 cycles	C-501	-	30	40	40	30	40	80	450
Specific Gravity	D-792	1.20	1.26	1.26	1.26	1.10	1.15	1.18	1.18
Base		Ester	Ester	Ester	Ester	Ether	Ether	Ether	Ether

Call us TOLL-FREE 1-800-343-4275 (outside CT)

HARKNESS Industries, Inc.

"Your Urethane Store"

50 Grandview Court, Cheshire, CT 06410  
Tel: 203-272-3219 • Fax: 203-272-0428



# Comparison of Hardness of polyurethane with natural and synthetic rubbers

		NITRILE (BUNA N) butadiene styrene acrylonitrile		SILICONE polyisobutylene polymer		VITON vinylidene fluoride and hexafluoropropylene		HYPOLAN chlorosulfonated polyethylene		HARNESS polyurethane	
PROPERTIES		SBR OR BUNA S butadiene styrene Isobutylene Isoprene	BUTYL	NEOPRENE chloroprene	Over 3000	Over 3000	Over 2000	Over 2000	Over 2500	Over 3000	5000-8500
TENSILE STRENGTH (psi)	Pure gum Black loaded stocks	Over 3000 Over 3000	Below 1800 Over 2000	Below 1000 Over 2000	Below 1500 Over 2000	Below 1000 Over 2000	Over 3000 Over 3000	Over 3000 Over 3000	Over 2000 Over 3000	Over 3000 Over 3000	Up to 75 Shoremeter D
HARDNESS RANGE (Shoremeter A)	30-90	40-50	40-75	40-95	40-85	40-95	40-95	60-95	40-95	40-95	50-99+
SPECIFIC GRAVITY (Base Material)	0.93	0.94	0.92	0.90	0.90	0.90	0.90	0.95	0.95	0.95	1.10 to 1.24
VULCANIZING PROPERTIES	Excellent	Excellent	Good	Excellent	Excellent	Excellent	Excellent	Good	Excellent	Excellent	Excellent
ADHESION TO METALS	Excellent	Excellent	Good	Excellent	Excellent	Excellent	Excellent	Good to excellent	Good	Good	Excellent
ADHESION TO FABRICS	Excellent	Good	Fair	Good	Fair	Poor	Good	Fair	Fair	Fair	Excellent
TEAR RESISTANCE	Good	Good	Good	Good	Good	Poor	Good	Fair	Fair	Fair	Outstanding
ABRASION RESISTANCE	Excellent	Good to excellent	Good	Good	Good	Poor	Excellent	Good	Excellent	Good	Outstanding
COMPRESSION SET	Good	Good	Fair	Good	Fair	Fair	Fair to Good	Very good	Fair	Fair	Good
REBOUND	Cold	Excellent	Good	Bad	Good	Excellent	Very Good	Good	Good	Good	Fair at low temp.
HDL	Excellent	Good	Very Good	Good	Good	Excellent	Very Good	Excellent	Good	Good	Good at room temp.
ELECTRIC STRENGTH	Excellent	Excellent	Excellent	Poor	Good	Good	Good	Good	Good	Good	Excellent
ELECTRICAL INSULATION	Good to excellent	Good to excellent	Poor	Poor	Excellent	Fair to Good	Fair to Good	Fair to Good	Fair to Good	Fair to Good	Excellent
PERMEABILITY TO GASES	Fair	Fair	Very low	Fair	Fair	Low	Very low	Low to very low	Low to very low	Low to very low	Fair to Good
ACID RESISTANCE	Good to Good	Good to Good	Excellent	Good	Excellent	Excellent	Excellent	Excellent	Excellent	Excellent	Fair to Good
Concentrated Aliphatic hydrocarbons	Fair to Good	Fair to Good	Excellent	Good	Fair	Good	Excellent	Very Good	Very Good	Very Good	Poor
Aromatic hydrocarbons	Poor	Poor	Poor	Excellent	Poor	Good	Excellent	Good	Good	Good	Excellent
OXYGENATED (ketones, etc.)	Good	Good	Good	Poor	Good	Poor	Poor	Poor	Poor	Poor	Fair to Good
Lacquer solvents	Poor	Poor	Poor	Poor	Fair	Poor	Poor	Poor	Poor	Poor	Poor
Water absorption	Poor	Poor	Poor	Very Good	Fair	Good	Excellent	Very Good	Very Good	Very Good	Good at room temp.
SWELLING IN LUBRICATING OIL	Poor	Poor	Poor	Excellent	Fair	Good	Excellent	Excellent	Excellent	Excellent	Excellent
Oil and gasoline	Poor	Poor	Poor	Excellent	Fair	Good	Excellent	Good	Good	Good	Fair at 175°F
Animal and vegetable oils	Poor to Good	Poor to Good	Excellent	Excellent	Fair	Good	Excellent	Good	Good	Good	Excellent
Oxidation	Very Good	Good to excellent	Very Good	Fair to Good	Good	Good	Very Good	Very Good	Very Good	Very Good	Outstanding
Ozone	Good	Good	Excellent	Fair	Excellent	Excellent	Excellent	Outstanding	Outstanding	Outstanding	Outstanding
Sunlight aging	Poor	Poor	Very Good	Poor	Excellent	Poor	Very Good	Very Good	Very Good	Very Good	Excellent
Heat aging	Good	Very Good	Excellent	Excellent	Outstanding	Excellent	Outstanding	Excellent	Excellent	Excellent	Good
Flame	Poor	Poor	Poor	Poor	Fair	Poor	Poor	Poor	Poor	Poor	Good
Heat	Good	Excellent	Excellent	Excellent	Excellent	Excellent	Excellent	Good	Good	Good	Good
Cold	Excellent	Excellent	Good	Excellent	Good	Good	Good	Good	Good	Good	Excellent